Polyhedron 55 (2013) 37–44

Contents lists available at SciVerse ScienceDirect

Polyhedron

journal homepage: www.elsevier.com/locate/poly

An iron(II) spin crossover grafted cyclotriphosphazene

Ross J. Davidson [a], Eric W. Ainscough [a,*], Andrew M. Brodie [a,*], Geoffrey B. Jameson [a], Mark R. Waterland [a], Boujemaa Moubaraki [b], Keith S. Murray [b], Keith C. Gordon [c], Raphael Horvath [c], Guy N.L. Jameson [c]

[a] *Chemistry – Institute of Fundamental Sciences, Massey University, Private Bag 11 222, Palmerston North 4442, New Zealand*
[b] *School of Chemistry, Building 23, Monash University, Clayton, Victoria 3800, Australia*
[c] *MacDiarmid Institute for Advanced Materials and Nanotechnology, Department of Chemistry, University of Otago, Dunedin 9054, New Zealand*

ARTICLE INFO

Article history:
Received 11 October 2012
Accepted 18 February 2013
Available online 5 March 2013

Keywords:
Cyclotriphosphazene
Iron(II)
Spin crossover

ABSTRACT

The synthesis of the new cyclotriphosphazene (CTP) ligand substituted with a pendant 2,6-bis(benzimidazole-2-yl)pyridine (bbp), namely (pentaphenoxy)[4-{2,6-bis(benzimidazole-2-yl)pyridine-4-yl}phenoxy]cyclotriphosphazene **L** is reported. The single crystal structure of **L** shows that the bbp group is attached to the CTP via the oxygen. **L** reacts with FeX_2 ($X = ClO_4^-$ or BF_4^-) salts forming the $[Fe\mathbf{L}_2]X_2$ complexes **1** and **2** respectively. For $[Fe\mathbf{L}_2](BF_4)_2$ (**2**), the single crystal structure shows an 'N_6' coordination sphere around the iron atom. UV–Vis, resonance Raman and Mössbauer spectroscopies and magnetic susceptibility measurements, aided by density functional theory (DFT) calculations, determine the complexes are low spin below 300 K but display spin crossover (SCO) behavior above this temperature, hence showing that the addition of a phosphazene to a SCO moiety does not prevent SCO.

1. Introduction

For many years, spin crossover (SCO) materials have been suggested as having potential for use in quantum computers and massive data storage systems for example [1,2]. However, because these materials are often crystalline, they are difficult and expensive to deposit and process. Previously we attempted to improve the processing properties by attaching pendant 2,2′:6′,2″-terpyridine (terpy) substituents to both cyclotri- and polyphosphazene (CTP and PP) (Scheme 1) and forming the subsequent iron(II) complexes [3]. The repeating nitrogen-phosphorus backbone provided an electronically mute scaffold for the metal–ligand centers; however, it was determined that only the start of SCO was observed at very high temperatures, preventing most practical applications [3].

The present study aims to improve on the terpy-based design by using a 2,6-bis(1*H*-benzimidazol-2-yl)pyridine (bbp) moiety attached to a CTP. The physical properties of the resultant iron(II) complexes were investigated using a variety of spectroscopic techniques, such as electronic absorbance, solid state resonance Raman and Mössbauer spectroscopy as well as magnetic susceptibility. DFT calculations were employed to obtain insight into the behavior of the compounds. Bbp was chosen, as iron(II)-bis-bbp ($[Fe(bbp)_2]^{2+}$) complexes are well known for their SCO behavior [4–8], thus should provide an improvement over terpy-based phosphazene complexes previously reported [3]. This is the first time phosphazene systems containing these imidazolyl-pyridyl species have been reported and it was of interest to determine if and how the substitution of the phosphazene alters their SCO behavior.

2. Experimental

Analytical grades of solvents were used. 2,6-bis(1*H*-benzimidazol-2-yl)pyridine-4(1*H*)-one (HObbp) [9] and 1,2,2,3,3-pentakis(phenoxy)-1-chlorocyclotriphosphazene, $N_3P_3(OPh)_5Cl$, [10] were synthesized by literature methods. K_2CO_3, $Fe(ClO_4)_2{\cdot}6H_2O$ and $Fe(BF_4)_2{\cdot}6H_2O$ were sourced from Aldrich–Sigma. To avoid iron(II) oxidation, all manipulations were carried out under an argon atmosphere, using standard Schlenk techniques.

Caution! Perchlorate salts with organic ligands are potentially explosive and should be handled with the necessary precautions.

2.1. Synthesis of the compounds

2.1.1. [$N_3P_3(OPh)_5(Obbp)$] (L)

$N_3P_3(OPh)_5Cl$ (195 mg, 0.31 mmol) was added to a solution containing HObbp (100 mg, 0.31 mmol) and K_2CO_3 (45 mg, 0.33 mmol) in acetone (50 mL). After stirring at reflux for five days the solvent was removed under reduced pressure, leaving a pink solid that was washed with $CHCl_3$/water and dried over $MgSO_4$. A minimal amount of hexane was added to the solution to form a white precipitate. The precipitate was filtered and dried under vacuum for elemental analysis. Diffractable crystals were grown via a slow evaporation of an acetone/water solution. Yield: 140 mg (51%).

---

* Corresponding authors. Tel.: +64 63569099; fax: +64 63505682.
E-mail addresses: e.ainscough@massey.ac.nz (E.W. Ainscough), a.brodie@massey.ac.nz (A.M. Brodie).

0277-5387/$ - see front matter © 2013 Elsevier Ltd. All rights reserved.
http://dx.doi.org/10.1016/j.poly.2013.02.065

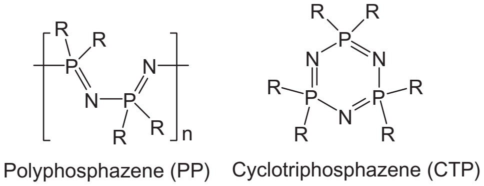

Scheme 1. Generic polyphosphazene (PP) and cyclotriphosphazene (CTP) structures.

ESMS: *m*/*z* 927 $[N_3P_3(OPh)_5(Obbp)H]^+$, 965 $[N_3P_3(OPh)_5(Obbp)K]^+$.$^{31}P\{^1H\}$ NMR ($CDCl_3$): δ 9.6 ppm (s). ^1H NMR ($CDCl_3$): δ 8.02 ppm (s, 2H), 7.40 (s, 2H), 7.05–7.00 (m, 10H), 6.95 (d (J = 8 Hz), 10H), 6.81 (t (8), 8H), 6.77 (d (8), 5H). *Anal.* Calc. for $C_{49}H_{37}N_8O_6P_3\cdot{}^2/_3CHCl_3$: C, 59.28; H, 3.77; N, 11.13. Found: C, 59.18; H, 3.76; N, 11.06%.

2.1.2. [Fe**L**₂](ClO₄)₂ (**1**)

To a stirred solution of **L** (100 mg, 0.11 mmol) in MeOH:$CHCl_3$ (1:1, 8 mL), $Fe(ClO_4)_2\cdot6H_2O$ (4.0 mg, 0.066 mmol) was added, immediately turning the solution purple. Stirring was continued for 30 min before the solvent was removed under reduced pressure. The solid was dissolved in $CHCl_3$ and filtered through Celite. The filtrate was dried under reduced pressure, leaving a purple solid. Weakly diffractable crystals were grown by dissolving the solid in acetone and diffusing in tert-butyl-methyl ether. Yield: 72 mg (62%). ESMS: *m*/*z* 955 $[Fe(L)_2]^{2+}$. $^{31}P\{^1H\}$NMR (CD_3CN): δ 11.28 ppm (d (93 Hz), 4P), −44.09 (t (93), 2P). ^1HNMR (CD_3CN): δ 14.48 ppm (4H), 9.00 (4H), 8.06 (4H), 7.85 (20H), 7.67 (10H), 7.57 (20H), 6.73 (4H), 6.32 (4H), 6.17 (4H). *Anal.* Calc. $C_{98}H_{74}Cl_2FeN_{16}O_{20}P_6\cdot C_5H_{12}O\cdot2H_2O$: C, 55.41, H, 4.06; N, 10.04. Found: C, 55.26; H, 4.01; N, 10.01%.

2.1.3. [Fe**L**₂](BF₄)₂ (**2**)

The same procedure as for **1** was used, except $Fe(BF_4)_2\cdot6H_2O$ was used in place of $Fe(ClO_4)_2\cdot6H_2O$. Diffractable crystals were grown by dissolving the solid in acetone and diffusing in tert-butyl-methyl ether. Yield: 70 mg (63%). ESMS: *m*/*z* 955 $[Fe(L)_2]^{2+}$. $^{31}P\{^1H\}$NMR (CD_3CN): δ 11.6 ppm (d (93 Hz), 4P), −41.9 (t (93), 2P). ^1HNMR (CD_3CN): δ 14.60 ppm (4H), 8.94 (4H), 8.04 (4H), 7.84 (20H), 7.61 (10H), 7.57 (20H), 6.84 (4H), 6.64 (4H), 6.11 (4H). *Anal.* Calc. $C_{98}H_{74}Cl_2FeN_{16}O_{20}P_6\cdot{}^3/_4C_5H_{12}O\cdot H_2O$: C, 56.39; H, 3.95; N, 10.34. Found: C, 56.34; H, 4.02: N, 10.39%.

2.2. Crystallographic studies

The X-ray data were collected at low temperature with a Rigaku-Spider X-ray diffractometer, comprising a Rigaku MM007 microfocus copper rotating-anode generator, high-flux Osmic monochromating and focusing multilayer mirror optics (Cu K radiation, λ = 1.5418 Å), and a curved image-plate detector. *CrystalClear* was utilized for data collection and *FSProcess* in *PROCESS-AUTO* was used for cell refinement and data reduction. Crystal refinement data are given in Table 1. The structures were solved by direct methods and refined using both the SHELXTL [11] and OLEX*2* [12] programs. Hydrogen atoms were calculated at ideal positions.

For the solution of $\mathbf{2}\cdot C_3H_6O\cdot C_5H_{12}O$, the electron density (15 e^- per cell in a void volume of 118.5 $Å^3$) of the occupationally and positionally disordered acetone molecule was removed by using PLATON/SQUEEZE [13].

2.3. Physical measurements

Microanalyses were performed by the Campbell Microanalytical Laboratory, University of Otago, New Zealand and assigned using *CHN* [14]. $^{31}P\{^1H\}$ NMR measurements were carried out on a Bruker Avance 400 spectrometer and ^1H NMR on a Bruker Avance 500 spectrometer. Electrospray mass spectra were obtained from acetonitrile solutions on a Micromass ZMD spectrometer run in the positive ion mode. Listed peaks correspond to the most abundant isotopomer; assignments were made by a comparison of observed and simulated spectra. All ground state vibrational measurements were made using KBr disks on a Nicolet 5700 FT-IR spectrometer. Continuous wave excitation was used for all Raman measurements. UV–Vis absorbance spectra were recorded using an Oceans Optics USB2000 + UV–Vis spectrophotometer on solutions prepared by dissolving the solid complexes in acetonitrile. Cyclic voltammetry was obtained using a glassy carbon working electrode, Pt counter electrode and Ag/AgCl reference electrode; v = 0.1 V s^{-1} recorded in acetonitrile, 0.1 M $TBAClO_4$ at 10^{-3} for the complexes **1**; 0.1 M $TBABF_4$ at 10^{-3} for **2**.

Table 1
Crystal and Refinement Data for $\mathbf{L}\cdot3H_2O\cdot C_3H_6O$ and $\mathbf{2}\cdot C_3H_6O\cdot C_5H_{12}O$.

Compound	$\mathbf{L}\cdot3H_2O\cdot C_3H_6O$	$\mathbf{2}\cdot C_3H_6O\cdot C_5H_{12}O$
Molecular formula	$C_{52}H_{49}N_8O_{10}P_3$	$C_{106}H_{92}B_2F_8FeN_{16}O_{14}P_6$
M (g mol^{-1})	1038.91	2229.26
T (K)	163(2)	123(2)
Crystal system	triclinic	triclinic
Space group	$P\bar{1}$	$P\bar{1}$
a (Å)	11.8419 (4)	12.880(3)
b (Å)	14.0379 (4)	17.690(4)
c (Å)	15.3918 (11)	24.070(5)
α (°)	91.665 (7)	85.16(3)
β (°)	90.322 (6)	83.21(3)
γ (°)	96.231 (2)	75.32(3)
V ($Å^3$)	2542.4 (2)	5259.6(21)
Z	2	2
μ (Cu Kα) (mm^{-1})	1.634	2.736
ρ_{calc} (g cm^{-3})	1.357	1.407
$2\theta_{max}$ (°)	117.88	102.26
Number of unique reflections	7193	11111
Data/restraints/parameters	7193/60/685	11111/2766/1494
Final R indices [$I > 2\sigma(I)$]	R_1 = 0.0756	R_1 = 0.0916
	wR_2 = 0.1775	wR_2 = 0.2155
R indices (all data)	R_1 = 0.1347	R_1 = 0.1137
	wR_2 = 0.2407	wR_2 = 0.2296
Goodness-of-fit (GOF) on F^2	1.074	0.967

Resonance Raman measurements were carried out based on a modified version of a system described previously [15–17]. Spectra were acquired of solid-state samples at 79, 298 and 362 K with a number of excitation wavelengths. Temperature control was achieved by utilizing a variable temperature cell (Specac, Woodstock, GA, USA) and a high stability temperature controller (Specac, Woodstock, GA, USA). Vacuum-purging of the cell was used to minimize condensation and frosting of the quartz window of the variable temperature cell. For excitation at 350.7 and 568.2 nm, a continuous-wave Innova I-302 krypton-ion laser (Coherent, Inc.) was used. For excitation at 457.9 and 514.5 nm an Innova Sabre DBW argon-ion laser (Coherent, Inc.) was used. The beam was passed through either a Pellin-Broca prism (for 350.7, 457.9 and 514.5 nm) or a holographic laser band pass filter (Kaiser Optical Systems, Inc.) and subsequently two irises in order to remove unwanted laser-lines. The beam-power was adjusted between 20 and 40 mW at the sample, depending on the wavelength used. The sample and collection lens were arranged in a 180° backscattering geometry where the collection lens also served to focus the excitation beam on the sample. The Raman photons were focused on the entrance slit of an Acton Research SpectraPro500i spectrograph (Princeton Instruments, Inc.) with a 1200 grooves mm^{-1} grating. The slit width was set to 50 µm, giving a resolution of ca. 2 cm^{-1}. Radiation from Raleigh and Mie-scattering was attenuated using a notch filter (Kaiser Optical Systems, Inc.) for 568.2 nm and Razor